

Mathematical Analysis of Added-Mass Instability in Fluid-Structure Interaction

Pongpat Thavornpattanapong, Kelvin Wong, Sherman C.P. Cheung and Jiyuan Tu

School of Aerospace, Mechanical and Manufacturing Engineering

RMIT University

Bundoora, VIC 3083, Australia

Tel.: +61-3-9925 6191, Fax: +61-3-9925 6108

Email: jiyuan.tu@rmit.edu.au

ABSTRACT

In solution procedure of fluid-structure interaction (FSI), the so-call artificial added mass effect plays an important role in determining the stability of the computation. We propose a derivation using Von Neumann stability analysis, which shows its significance as a tool for studying this numerical instability. Our derivation demonstrates that FSI solution is severely unstable when density ratio is high, solid structure is thin and flexible. It also shows that this instability can be eliminated by introducing artificial compressibility.

Keywords: Fluid-Structure Interaction, Added Mass Instability, Artificial Compressibility, Automotive, Von Neumann Stability Analysis.

1 Introduction

It is well known that flow-induced vibration analysis can be done in mainly two approaches: Monolithic and Partitioned frameworks. The monolithic approach solves a system of governing equations of both fluid and solid fields (Hron and Turek, 2006). Although this monolithic approach gives strong coupling between the fields, it is impractical for real world engineering applications. This is not only because of its very demanding computational power for solving such a large system of equations but also the need of development preconditioning. The partitioned approach is attractive due to its advantage of software modularity allowing selection of an appropriate solver among well-established solvers for each field. However, there is still needs for improvement of the efficiency of partitioned approach, especially for applications involves with large deformation because of the added-mass instability. This instability usually occurs in problem with large deformation and light weight structure. To eliminate this instability, extremely small values of coupling relaxation factors of interface loads must be used. This leads to a significant increase in computational time. Many researchers have been searching for technique to deal with this instability. (Kuttler and Wall, 2008) employed adaptive relaxation techniques, such as the Aitken and Steepest descent relaxation, to increase speed of calculation. The general idea of adaptive relaxation is to use the information about earlier iterations to approximate a value of relaxation, which likely to provide stability. Another alternative

is the so-called reduced model developed by (Degroote, Bathe and Vierendeels, 2009). “Interface artificial compressibility” was implemented in a commercial software package, ADINA. In this particular framework, it is proved that the stability of FSI solution can be improved significantly. For many decades, artificial compressibility has been utilized as a tool to stabilize coupling between momentum and continuity equations when solving incompressible flows (Chorin, 1967). Recently, it was first used for stabilization of FSI problems in (Raback, Ruokolainen and M. Lyly, 2001). In his paper, the method of applying this technique by introducing an additional source term in continuity equation is explained.

Numerous papers by (Causin, Gerbeau and Nobile, 2005) have been published in attempt to provide a clear demonstration of the reasons why this instability is crucial and has to be treated carefully. This paper serves as an alternative of derivation of the problem using Von Neumann stability analysis. This method can demonstrate how the conditions of each problem affect stability of solution. Moreover, it is illustrated how application of artificial compressibility helps stabilize system of FSI solution.

2 Mathematical Analysis of Artificial Added-Mass Instability

In this section, the instability of fluid-structure interaction using partitioned approach is discussed. This section is divided into two sub-sections. The first one is the derivation of instability which occurs when using Leap-Frog and forward Euler schemes without artificial compressibility. The second one is the derivation of instability which occurs when using Leap-Frog and forward Euler schemes with artificial compressibility.

2.1 Leap-Frog and Euler scheme

We refer to governing equation of deformation of a flexible cylindrical tube in (Causin et al., 2005), which can be written as

$$\rho_s h_s \frac{\partial^2 d_\Gamma^s}{\partial t^2} + \rho_f M_a \frac{\partial^2 d_\Gamma^f}{\partial t^2} + a_0 d_\Gamma^s - b \frac{\partial^2 d_\Gamma^s}{\partial x^2} = P_{ext,\Gamma}, \quad (2.1)$$

where $a_0 = \frac{E h_s}{r^2(1-\nu^2)}$ and $b = K_T B h_s$.

The Leap-Frog scheme for structural acceleration is written as

$$\ddot{d}_\Gamma^{n+1,s} = \frac{1}{\Delta t^2} (d_\Gamma^{n+1} - 2d_\Gamma^n + d_\Gamma^{n-1}). \quad (2.2)$$

The Euler scheme for FSI interface acceleration for fluid domain is written as

$$\dot{d}_\Gamma^{n+1,f} = \frac{1}{\Delta t} (\dot{d}_\Gamma^n - \dot{d}_\Gamma^{n-1}) = \frac{1}{\Delta t^2} (d_\Gamma^n - 2d_\Gamma^{n-1} + d_\Gamma^{n-2}). \quad (2.3)$$

It is noted that superscript m represents pseudo time step or stagger iteration, while n represents physical time step. Also, x and t are space and time respectively.

Due to the nature of sequential approach, the information used for calculation of FSI interface acceleration for fluid domain is always one step behind solid. From (2.1), since we are interested in added-mass instability, where the mass term is dominated the stiffness term, we will neglect some non-linearity. Therefore, (2.1) is reduced to equation (2.4) such that

$$\rho_s h_s \frac{\partial^2 d_\Gamma^s}{\partial t^2} + \rho_f M_a \frac{\partial^2 d_\Gamma^f}{\partial t^2} + a_0 d_\Gamma^s = P_{ext,\Gamma}. \quad (2.4)$$

Discretization of (2.4) is achieved by substituting (2.2) and (2.3) to give

$$\frac{\rho_s h_s}{\Delta t^2} (d_\Gamma^{n+1} - 2d_\Gamma^n + d_\Gamma^{n-1}) + \frac{\rho_f M_a}{\Delta t^2} (d_\Gamma^n - 2d_\Gamma^{n-1} + d_\Gamma^{n-2}) + a_0 d_\Gamma^n = P_{ext,\Gamma}^n. \quad (2.5)$$

To simplify it, let's look at only one position on the interface. Notice that the added-mass operator M_A can be represented by the i th eigenvalues of M_A , μ_i . This make (2.5) reduced further to (2.6) as given by

$$\frac{\rho_s h_s}{\Delta t^2} (d_i^{n+1} - 2d_i^n + d_i^{n-1}) + \frac{\rho_f \mu_i}{\Delta t^2} (d_i^n - 2d_i^{n-1} + d_i^{n-2}) + a_0 d_i^n = P_{ext,i}^n. \quad (2.6)$$

Next we will use the idea of Von Neumann stability analysis to prove stability of the system of discrete equation (Strang, 2007). This technique based on understanding in fourier analysis that any function can be represented by a superposition of basis functions like sine, cosine and exponential functions. The idea is to represent the solution in term of initial value $e^{iat} e^{ikx}$, which depends only on spatial variation x . In other words, we are trying to separate variables x and t in our solution. This will allow us to monitor how the solution is growing with time. Initial value of solution can be written as

$$d(x, t) \approx \int_{-\infty}^{\infty} e^{iat} e^{ikx} dk$$

or

$$d(x, t) \approx \sum_{-\infty}^{\infty} e^{iat} e^{ikx}. \quad (2.7)$$

Note that a is a temporal wave frequency, which is also a function of spatial wave frequency, k . For simplicity, we drop the summation sign in equation (2.7) since our aim is to prove the instability, which can be done by monitoring only one mode of the solution. Therefore (2.7) becomes

$$d(x, t) \approx e^{iat} e^{ikx}. \quad (2.8)$$

Now we have separated the time and space variation in our solution. From (2.8), the initial solution is in the form of multiplication of complex exponential terms and our initial value $e^{iat} e^{ikx}$. The next step is to represent the other terms (d_i^n , d_i^{n-1}) in term of the initial value of the system (d_i^{n-2}). This is set to be the initial value because in the discrete equation (2.6), d_i^{n-2} is the oldest information available.

Let $d_i^{n-2} \approx e^{iat} e^{ikx}$, which is our initial value. Therefore, displacement at time step $n - 1$ and n can be represented as

$$d_i^{n-1} = e^{ia(t+\Delta t)} e^{ikx} \quad \text{and} \quad d_i^n = e^{ia(t+2\Delta t)} e^{ikx}.$$

By substituting (2.9) into (2.6), we get

$$\begin{aligned} \frac{\rho_s h_s}{\Delta t^2} (d_i^{n+1} - 2e^{ia(t+2\Delta t)} e^{ikx} + e^{ia(t+\Delta t)} e^{ikx}) + \frac{\rho_f \mu_i}{\Delta t^2} (e^{ia(t+2\Delta t)} \\ - 2e^{ia(t+\Delta t)} e^{ikx} + e^{ikx}) + a_0 e^{ia(t+2\Delta t)} e^{ikx} = P_{ext,i}^n. \end{aligned} \quad (2.9)$$

The growth factor is determined by rearranging above equation as

$$\begin{aligned} d_i^{n+1} &= \left\{ \frac{\Delta t^2}{\rho_s h_s} \left[\frac{P_{ext,i}^n}{e^{iat} e^{ikx}} - a_0 e^{ia2\Delta t} - \frac{\rho_f \mu_i}{\Delta t^2} (e^{ia2\Delta t} - 2e^{ia\Delta t} + 1) \right] + 2e^{ia2\Delta t} - e^{ia\Delta t} \right\} e^{iat} e^{ikx} \\ &= \left\{ -\frac{\rho_f \mu_i}{\rho_s h_s} (e^{ia2\Delta t} - 2e^{ia\Delta t} + 1) + 2e^{ia2\Delta t} - e^{ia\Delta t} \right\} e^{iat} e^{ikx} \quad \because \Delta t^2 \rightarrow 0 \\ &= \left\{ -\frac{\rho_f \mu_i}{\rho_s h_s} e^{ia2\Delta t} + 2\frac{\rho_f \mu_i}{\rho_s h_s} e^{ia\Delta t} - \frac{\rho_f \mu_i}{\rho_s h_s} + 2e^{ia2\Delta t} - e^{ia\Delta t} \right\} e^{iat} e^{ikx} \\ &= \underbrace{\left\{ \left[-\frac{\rho_f \mu_i}{\rho_s h_s} + 2 \right] e^{ia2\Delta t} + \left[2\frac{\rho_f \mu_i}{\rho_s h_s} - 1 \right] e^{ia\Delta t} - \frac{\rho_f \mu_i}{\rho_s h_s} \right\}}_{\text{Growth Factor}} \underbrace{e^{iat} e^{ikx}}_{\text{Initial value}}. \end{aligned} \quad (2.10)$$

The solution is unstable if the absolute value of growth factor is greater than 1. Therefore, instability occurs if (2.11) that is given as

$$\left| \left[-\frac{\rho_f \mu_i}{\rho_s h_s} + 2 \right] e^{ia2\Delta t} + \left[2\frac{\rho_f \mu_i}{\rho_s h_s} - 1 \right] e^{ia\Delta t} - \frac{\rho_f \mu_i}{\rho_s h_s} \right| > 1 \quad (2.11)$$

is satisfied.

Although the growth factor we have here is an accumulated growth over three time step, it gives us enough information for determining if the solution of considered system is stable or not. This is because if growth factor after three time steps and the corresponding growth factor after one time step will still result in the same condition. A graphical representation of (2.11) can be plotted in a complex plane and compared with a unit circle in order to demonstrate the instability of the current scheme used for FSI as illustrated in Figures 1. The origin of a circle related to this growth factor is shifted by $-\frac{\rho_f \mu_i}{\rho_s h_s}$ in the real axis of the complex plane. The radius is $\left| \left[-\frac{\rho_f \mu_i}{\rho_s h_s} + 2 \right] + \left[2\frac{\rho_f \mu_i}{\rho_s h_s} - 1 \right] \right|$, which equal to $\left| \frac{\rho_f \mu_i}{\rho_s h_s} + 1 \right|$. This is because $e^{ia\Delta t}$ and $e^{ia2\Delta t}$ are both equivalent to a unit circle.

It is clear that if $\frac{\rho_f \mu_i}{\rho_s h_s}$ is greater than or equivalent to zero, the FSI solution using Leap-Frog and Euler scheme becomes unstable. It can be concluded that the explicit scheme is unconditionally unstable. It is shown in Figures 1 that physical properties of engineering problem being solved are crucial to stability of the solution.

2.2 Leap-Frog and Euler scheme with artificial compressibility

According to (Degroote et al., 2009), artificial compressibility can be successfully used to enhance stability of the system. He claims that the artificial compressibility term introduced to the

system helps stabilize the solution by mimic the information transferred across the interface as shown in (2.12) to (2.19).

The simplified fluid governing equation is written as

$$\frac{\partial V_m^{n+1}}{\partial t} + \int_{\partial V^n} (v_{m+1}^{n+1} - v_b^n) dA = 0. \quad (2.12)$$

After introducing artificial compressibility, (2.12) becomes

$$\text{Artificial compressibility term} + \frac{\partial V_m}{\partial t} + \int_{\partial V^n} (v_{m+1}^{n+1} - v_b^n) dA = 0, \quad (2.13)$$

$$\int \frac{1}{\rho c^2} \frac{p_{m+1}^{n+1} - p_m^{n+1}}{\Delta t} dV + \frac{\partial V_m^{n+1}}{\partial t} + \int_{\partial V_m} (v_{m+1}^{n+1} - v_b^n) dA = 0. \quad (2.14)$$

According to (Degroote et al., 2009),

$$c^2 = \frac{p_b - p_a \text{ vol}}{\Delta \text{vol} \rho}. \quad (2.15)$$

By substituting (2.15) in (2.14), we get

$$\frac{\Delta \text{vol}}{p_b - p_a} \frac{p_{m+1}^{n+1} - p_m^{n+1}}{\Delta t} + \frac{\partial V_m^{n+1}}{\partial t} + \int_{\partial V_m} (v_{m+1}^{n+1} - v_b^n) dA = 0. \quad (2.16)$$

To simplify,

$$\frac{\Delta \text{vol}}{p_b - p_a} \frac{p_{m+1}^{n+1} - p_m^{n+1}}{\Delta t} \approx \frac{\Delta \text{vol}}{\Delta t} \approx \frac{V_{m+1}^{n+1} - V_m^{n+1}}{\Delta t}. \quad (2.17)$$

$$\frac{\partial V_m}{\partial t} = \frac{V_m^{n+1} - V_m^n}{\Delta t}. \quad (2.18)$$

For validation of (2.16), we refer to (Degroote et al., 2009).

Substituting (2.17) and (2.18) in (2.16), we get

$$\frac{\partial V_m^{n+1}}{\partial t} + \int_{\partial V^n} (v^{n+1} - v_b^n) dA = 0. \quad (2.19)$$

Therefore, It might be reason able to use $\ddot{d}_{m+1}^{n+1,f} = \frac{1}{\Delta t^2} (d_{m+1,i}^{n+1} - 2d_{m,i}^{n+1} + d_{m-1,i}^{n+1})$ instead of $\ddot{d}_{m+1}^{n+1,f} = \frac{1}{\Delta t^2} (d_{m,i}^{n+1} - 2d_{m-1,i}^{n+1} + d_{m-2,i}^{n+1})$.

By conducting a similar Von Neumann stability analysis that we have done for Leap-frog and Euler scheme, but this time with artificial compressibility, we obtain

$$\frac{\rho_s h_s}{\Delta t^2} (d_i^{n+1} - 2d_i^n + d_i^{n-1}) + \frac{\rho_f \mu_i}{\Delta t^2} (d_i^{n+1} - 2d_i^n + d_i^{n-1}) + a_0 d_i^n = P_{ext,i}^n \quad (2.20)$$

$$d_i^{n+1} - 2d_i^n + d_i^{n-1} = \frac{\Delta t^2 (P_{ext,i}^n - a_0 d_i^n)}{\rho_s h_s + \rho_f \mu_i} \quad (2.21)$$

$$d_i^{n+1} - 2d_i^n + d_i^{n-1} = 0 \because \Delta t^2 \rightarrow 0. \quad (2.22)$$

It can be further reduced to

$$d_i^{n+1} = 2d_i^n - d_i^{n-1}. \quad (2.23)$$

By recalling (2.9),

$$d_i^{n-1} = e^{ia(t+\Delta t)} e^{ikx} \quad \text{and} \quad d_i^n = e^{ia(t+2\Delta t)} e^{ikx}.$$

Substituting into (2.23), we get

$$d_i^{n+1} = \left(2e^{ia2\Delta t} - e^{ia\Delta t}\right) e^{iat} e^{ikx}, \quad (2.24)$$

and

$$|G| = \left|2e^{ia2\Delta t} - e^{ia\Delta t}\right|. \quad (2.25)$$

The growth factor in (2.25) is equivalent to a unit circle with origin at (0,0) in a complex plane. Therefore, it is determined that solution is unconditionally stable when applying artificial compressibility.

3 Conclusion

In conclusion, explicit calculation of fluid-structure interaction leads to unconditional instability. On the contrary, previous studies have demonstrated that calculation in implicit way can result in conditional stability. Our derivation also shows that properties of problem such as density ratio and the flexibility of the solid structure can influence the stability significantly. Moreover, it is demonstrated that stability of the coupling can be maintained by applying “Artificial compressibility” technique. This numerical manipulation allows the solution to be done explicitly, which therefore reduces the computational time required to solve FSI problems.

Nomenclature

Solid density	ρ_s
Fluid density	ρ_f
Thickness of flexible tube	h_s
Displacement at interface	Γ
Displacement at i node (on interface)	d_i
Added-mass operator matrix	M_a
Time	t
Spatial coordinate	x
Fluid load on interface	Γ
Fluid load on interface at pseudo time n	$P_{ext,\Gamma}^n$
Fluid load at node i at pseudo time n	$P_{ext,i}^n$
Structural acceleration	\ddot{d}
Velocity	v
Grid Velocity	v_b
Eigen value of the added-mass operator	μ
Structural displacement	d
Reference radius of flexible cylindrical tube	r
Area	A
Volume	V
Pseudo time step level (coupling iteration)	m
Physical time step level	n
Pressure	P
Upper limit of expected pressure	P_a
Lower limit of expected pressure	P_b
Young modulus	E
Shear stress modulus	B
Poisson coefficient	ν
Timoshenko shear correction factor	K_T
Speed of sound	c
Growth factor	G
Real part of complex growth factor	$Re(G)$
Imaginary part of complex growth factor	$Im(G)$
Radius of growth factor	R

Acknowledgment

This original research was supported by the Commonwealth of Australia, through the Co-operative Research Centre for Advanced Automotive Technology (Project: Developing Numerical Model for Flow-Induced Vibration Excitation Mechanisms towards Virtual Laboratory Simulation,C4-503).

References

- Causin, P., Gerbeau, J.-F. and Nobile, F. 2005. Added-mass effect in the design of partitioned algorithms for fluid-structure problems., *Computer Methods in Applied Mechanics and Engineering* **194**(42-44): 4506–4527.
- Chorin, A. 1967. A numerical method for solving incompressible viscous flow problems., *Journal of Computational Physics* **2**: 1226.
- Degroote, J., Bathe, K.-J. and Vierendeels, J. 2009. Simulation of fluid-structure interaction with the interface artificial compressibility method, *International Journal for Numerical Methods in Biomedical Engineering* **26**: 276–289.
- Hron, J. and Turek, S. 2006. A monolithic fem/multigrid solver for ale formulation of fluid structure interaction with application in biomechanics., *FluidStructure Interaction Modelling, Simulation, Optimisation* **53**: 146–170.
- Kuttler, U. and Wall, W. 2008. Fixed-point fluid-structure interaction solvers with dynamic relaxation, *Computational Mechanics* **43**(1): 61–72.
- Raback, P., Ruokolainen, J. and M. Lyly, E. J. 2001. Fluid-structure interaction boundary conditions by artificial compressibility, *European Conference on Computational Fluid Dynamics ECCOMAS* .
- Strang, G. 2007. *Computational Science and Engineering*, Wellesley-Cambridge Press, USA.

List of figures

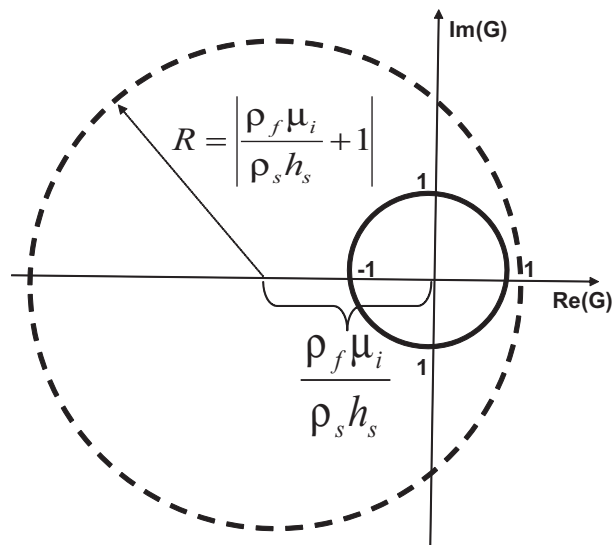


Figure 1: $\frac{\rho_f \mu_i}{\rho_s h_s} > 0, R > 1$ (Unconditionally unstable)